PHYSICAL REVIEW A **77**, 061602(R) (2008)

Spatial coherent transport of interacting dilute Bose gases

M. Rab,[1] J. H. Cole,[1,2] N. G. Parker,[1] A. D. Greentree,[1,2] L. C. L. Hollenberg,[1,2] and A. M. Martin[1]
[1]*School of Physics, University of Melbourne, Parkville, Victoria 3010, Australia*
[2]*Centre for Quantum Computer Technology, School of Physics, University of Melbourne, Parkville, Victoria 3010, Australia*
(Received 7 November 2007; published 4 June 2008)

We investigate coherent atomic tunneling of a dilute gas Bose-Einstein condensate (BEC) in a three-well system. In particular, we generalize stimulated Raman adiabatic passage (STIRAP) to adiabatically transport a BEC of 2000 ^{7}Li atoms between two wells with minimal occupation in the intervening well. This protocol paves the way for a robust method of control in atom-optical devices.

DOI: 10.1103/PhysRevA.77.061602 PACS number(s): 03.75.−b, 07.77.−n

Classically it is impossible to have transport without transit, i.e., if the points 1, 2, and 3 lie sequentially along a path then an object moving from 1 to 3 must, at some point in time, be located at 2. For a quantum particle in a three-well system it is possible to transport the particle between wells 1 and 3 such that the probability of finding it at *any time* in the classically accessible state in well 2 is negligible. We consider theoretically the analogous scenario for an interacting Bose-Einstein condensate (BEC). Specifically, the adiabatic transportation of a condensate of 2000 ^{7}Li atoms from well 1 to well 3 without a macroscopic occupation of the classically allowed intermediate well is predicted. Such a protocol paves the way for a robust method of control for atom-optical devices.

The ideas underpinning the protocol for macroscopic matter-wave transport without transit (TWT) stem from stimulated Raman adiabatic passage (STIRAP) [1–4]. STIRAP is a robust technique for transferring population between two atomic states, $|1\rangle$ and $|3\rangle$, via an intermediate excited state, $|2\rangle$. Using electromagnetic pulses to couple states $|1\rangle$ to $|2\rangle$ and $|2\rangle$ to $|3\rangle$, characterized by coupling parameters K_{12} and K_{23}. When K_{23} precedes and overlaps K_{12}, the population is adiabatically transferred from state $|1\rangle$ to $|3\rangle$. Population transfer is achieved via a superposition of states $|1\rangle$ and $|3\rangle$ with the occupation of state $|2\rangle$ strongly suppressed. These techniques are used in quantum optics for coherent internal state transfer [4–7] and have been proposed [8], and recently demonstrated [9], in three channel optical waveguides. Recently this protocol has been proposed to transport single atoms [10,11], Cooper pairs [12], spin states [13], and electrons [14–18] and is referred to as coherent tunneling adiabatic passage (CTAP). Here we consider transport of dilute gas BECs containing thousands of interacting atoms, thus distinguishing our treatment from the previous single particle cases.

The system under consideration is schematically shown in Fig. 1(a), where a three-dimensional harmonic trap is split into three regions via the addition of two parallel repulsive Gaussian potentials. With the Bose-Einstein condensate (BEC) initially in well 1, we show how, through adiabatic changes to the tunneling rates between the wells, to transport it into well 3 with minimal occupation of the intervening well. This effect is shown in Fig. 1(b), where a BEC of 2000 ^{7}Li atoms is transported from well 1 to well 3 over a timescale of ~1 s, with less than 1% of the atoms occupying well 2 at any time. As such it appears that the BEC is transported from well 1 to well 3 without macroscopically transiting through well 2.

Here we elucidate the properties of the three-well system by first considering a three-mode approximation [19–21], where the form of the potential is not important. We then employ the mean-field Gross-Pitaevskii equation (GPE) to quantitatively describe the BEC dynamics and consider experimental scenarios in which to realize macroscopic matter-wave TWT.

Reducing our three-well system, shown in Fig. 1(a), such that each well is described by a single mode basis [19–21], Ψ_i, gives

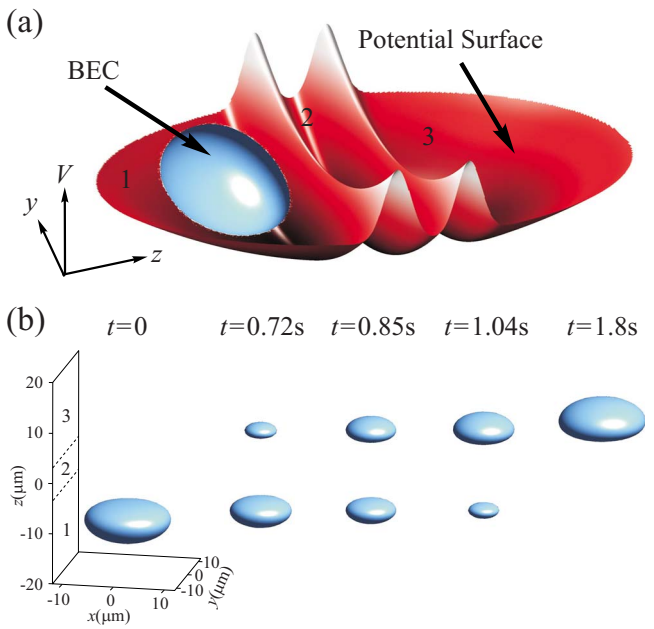

FIG. 1. (Color online) Macroscopic matter-wave transport without transit of a BEC in a three-well system. (a) Schematic representation of our system at $t=0$ in the $(z\text{-}y)$ plane. Two parallel, repulsive Gaussian barriers embedded in an ambient harmonic trap divide the system into three wells, with the BEC initially occupying well 1. (b) Isosurface plots of atomic density ($n_{\mathrm{iso}}=0.1n_0$, where n_0 is the initial peak density of the BEC) showing the adiabatic transportation of a BEC of 2000 ^{7}Li atoms over a distance of 20 μm [simulated using the three-dimensional (3D) Gross-Pitaevskii equation].

$$\Psi(t) = \psi_1(t)\Psi_1 + \psi_2(t)\Psi_2 + \psi_3(t)\Psi_3, \tag{1}$$

where

$$\frac{i}{\Omega_{\max}}\frac{\partial}{\partial t}\begin{pmatrix}\psi_1\\ \psi_2\\ \psi_3\end{pmatrix} = \begin{pmatrix}U_1 & -K_{12} & 0\\ -K_{12} & U_2 & -K_{23}\\ 0 & -K_{23} & U_3\end{pmatrix}\begin{pmatrix}\psi_1\\ \psi_2\\ \psi_3\end{pmatrix}. \tag{2}$$

The amplitude of each mode is expressed as $\psi_i = \sqrt{N_i}e^{i\theta_i}$, where N_i and θ_i are the occupation and phase of the ith mode, respectively $(i=1,2,3)$, and $\Sigma_{i=1}^{3}N_i(t)=N_T$, where N_T is the total number of atoms in the system. The parameters K_{ij} describe the tunneling rates between wells i and j. The dimensionless on-site interaction energy per particle is $U_i = E_i^0 + g_m N_i/N_T$, where E_i^0 is the ground-state energy of well i and g_m parametrizes the nonlinear atomic interactions within the system [22].

The modulation of the tunneling rates K_{12} and K_{23} effects the transfer of atoms between the wells. We assume these parameters vary with time as,

$$K_{12}(t) = \sin^2[\pi t/(2t_{\rm p})], \quad K_{23}(t) = \cos^2[\pi t/(2t_{\rm p})] \tag{3}$$

for $t \in [0, t_p]$, where $t_{\rm p}$ is the total pulse time and the maximum tunneling rate is $\Omega_{\max}$. We employ this pulsing scheme due to its robustness against nonlinear effects arising from the interatomic interactions at $t=0$ and $t=t_{\rm p}$. In the adiabatic limit $t_{\rm p}\to\infty$ and for $g_m=0$ the eigenmode evolution is [15],

$$D_+ = \sin\Theta_1 \sin\Theta_2\Psi_1 + \cos\Theta_2\Psi_2 + \cos\Theta_1 \sin\Theta_2\Psi_3,$$

$$D_- = \sin\Theta_1 \cos\Theta_2\Psi_1 - \sin\Theta_2\Psi_2 + \cos\Theta_1 \cos\Theta_2\Psi_3,$$

$$D_0 = \cos\Theta_1\Psi_1 - \sin\Theta_1\Psi_3, \tag{4}$$

where

$$\Theta_1 = \arctan[K_{12}/K_{23}]$$

$$\Theta_2 = \frac{1}{2}\arctan[(2\sqrt{K_{12}^2 + K_{23}^2})/E_2^0]. \tag{5}$$

The corresponding mode energies are shown in Fig. 2(a). For an initial state where all of the atoms are in well 1, the system adiabatically follows the green/middle line. In the adiabatic limit, this corresponds to the passage of atoms from well 1 to well 3, with zero occupation of well 2, as shown in Fig. 2(b), corresponding to ideal TWT, i.e. the current into well 2 from well 1 $[j_{12}(t)]$ is always equal to the current out of well 2 into well 3 $[j_{23}(t)]$.

Figures 2(a) and 2(b) are in an ideal limit where the atomic interactions are zero $(g_m=0)$ and the time over which the pulses were applied was long $(t_p\to\infty)$. For a realistic system we must examine how the ideal changes as the pulse times $(t_{\rm p})$ are reduced and interactions are included [19]. In particular, it is expected that away from the idea limit that $j_{12}(t) \neq j_{23}(t)$, resulting in a nonzero occupation of well 2. Hence, we classify the fidelity of the protocol via the fraction of atoms in well 3 at the end of the protocol, $N_3(t_{\rm p})/N_T$, and the maximum number of atoms occupying well 2 during the protocol, $\max[N_2(t)/N_T]$. These quantities are shown in Figs. 2(c) and 2(d), respectively, as a function of the strength of the nonlinear interactions g_m and the pulse time t_p, with efficient TWT occurring in the white regions. Defining the fidelity, ϵ, for TWT through $N_3(t_{\rm p})/N_T > \epsilon$ and $\max[N_2(t)/N_T] < 1-\epsilon$ to achieve $\epsilon \geq 0.99$ requires that $|g_m| < E_2^0 - E_1^0$ and $t_{\rm p}\Omega_{\max} \gtrsim 400$. In the absence of nonlinear interactions $(g_m=0)$ the condition $t_{\rm p}\Omega_{\max} > 400$ comes from the adiabatic limit of the system and is governed by the energy difference between the ground-state energies of the wells. As noted by Graefe *et al.* [19], the introduction of nonlinear interactions introduces nonlinear "eigenstates," which can inhibit adiabatic transfer. Reference [19] considered a Gaussian tunneling scheme, however, the sinusoidal protocol [Eq. (3)] is much more robust to nonlinear effects, since the energies of the additional nonlinear states are not close to the dark state mediating the transfer.

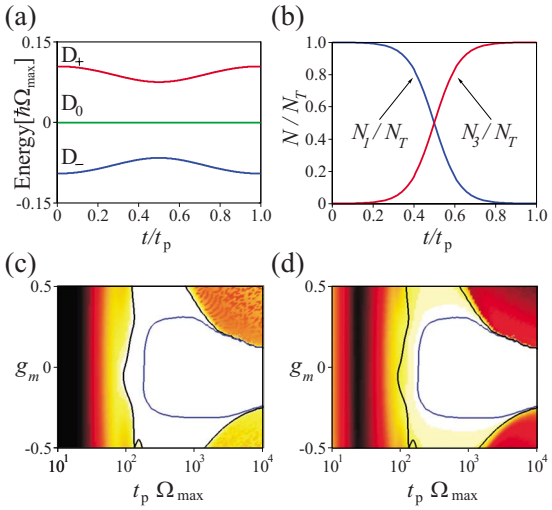

FIG. 2. (Color online) System dynamics according to three-mode analysis. (a) Energies of the eigenmodes D_+, D_0, and D_- of the noninteracting $(g_m=0)$ system. (b) Evolution of $N_1(t)/N_T$ and $N_3(t)/N_T$ for $g_m=0$ and $t_{\rm p}\to\infty$. (c) $N_3(t_{\rm p})/N_T$ as a function of g_m and t_p, with white and black representing $N_3(t_{\rm p})/N_T=1$ and 0, respectively. (d) $\max[N_2(t)/N_T]$ as a function of g_m and $t_{\rm p}$, with white and black representing $N_2(t_{\rm p})/N_T=0$ and 1, respectively. In (c) and (d) the solid black and blue/gray curves represent $N_3(t_{\rm p})/N_T=0.99$ and $\max[N_2(t)/N_T]=0.01$, respectively, and the region bounded by both corresponds to high fidelities $\epsilon \geq 0.99$. We have assumed $E_1^0 = E_3^0 = 0$ and $E_2^0 = 0.1\hbar\Omega_{\max}$ throughout.

The mode analysis presented above gives a qualitative description of adiabatic transport for a three-well system. To investigate TWT quantitatively for realistic scenarios, the GPE is employed to describe the evolution of the mean-field wave function, $\Psi(\mathbf{r},t)$, via

$$i\hbar\frac{\partial\Psi}{\partial t} = \left[-\frac{\hbar^2}{2m}\nabla^2 + V(\mathbf{r},t) + g|\Psi|^2\right]\Psi, \tag{6}$$

where $g = 4\pi\hbar^2 a/m$ is directly related to the strength of the nonlinear interactions used in the mode analysis (g_m), with a being the s-wave scattering length characterizing the atomic interactions in the BEC and m is the mass of the constituent atoms. As compared to the three mode analysis, solving the GPE includes the effects of (i) all the modes in the system;

(ii) the change of the ground-state energies of the wells as a function of the tunneling rates; and (iii) the spatial extent of the BEC wave function. The trapping potential we consider is

$$V(\mathbf{r},t) = \frac{m}{2}[\omega_\perp^2(x^2+y^2)+\omega_z^2 z^2] + V_{12}(t)e^{-(z+z_0)^2/(2\sigma^2)} + V_{23}(t)e^{-(z-z_0)^2/(2\sigma^2)}. \quad (7)$$

The first term defines the cylindrically symmetric parabolic trap with radial and axial trap frequencies $\omega_\perp$ and ω_z, respectively. The second and third terms represent repulsive Gaussian barriers at $z=\pm z_0$, with width σ and time-dependent amplitudes $V_{12}(t)$ and $V_{23}(t)$. Such barrier potentials can be induced by the optical dipole force from two parallel blue-detuned laser beams [23] or using magnetic fields on an atom chip [24]. The barrier amplitudes, which can be varied by modifying the laser intensity or the atom chip currents, control the tunneling rates between neighboring wells.

Recall that in the mode analysis we employed tunneling rates which initially had opposing values [Eq. (3)]. Due to difficulties in initializing such a state in an experiment and simulation, our simulations begin with barriers of identical height $V_{\max}$, and therefore initially identical tunneling rates. Over time, the barriers are smoothly lowered to a minimum value $V_{\min}$ before being returned to $V_{\max}$, such that the tunneling rate variation approximates a Gaussian [25]. Importantly, there is a time delay of size τ between the pulsing of $V_{12}(t)$ and $V_{23}(t)$. By analogy to conventional STIRAP, when $V_{12}(t)$ is pulsed before $V_{23}(t)$, we term this the *intuitive* protocol, and when $V_{12}(t)$ is pulsed after $V_{23}(t)$, we term this the *counter-intuitive* protocol. Only the latter is capable of producing TWT and so we concentrate on this.

Despite the qualitatively different TWT protocols for the mode analysis and GPE simulations, we see qualitative agreement in the regions of high fidelity [25]. This suggests that TWT is not particularly dependent on the exact form of $V_{12}(t)$ and $V_{23}(t)$ [$K_{12}(t)$ and $K_{23}(t)$], as expected for an adiabatic protocol. This has been verified through the study of several different functional forms for $V_{12}(t)$ and $V_{23}(t)$ [$K_{12}(t)$ and $K_{23}(t)$] which all produce qualitatively similar results.

The one-dimensional equivalent of the GPE can be solved numerically with relative ease and so we consider this limit first. Employing harmonic oscillator units, we consider a system defined by $\sigma=0.16 l_{\rm ho}=0.16\sqrt{\hbar/m\omega_z}$, $z_0=3\sigma$ and $\tau=t_p/10$. Figures 3(a) and 3(b) show the evolution of the condensate density $|\Psi(z)|^2$ for different time pulses but the same remaining parameters ($g_{1D}=0.31$, $V_{\min}=5\,\hbar\omega_z$ and $V_{\max}=10^4\,\hbar\omega_z$). In Fig. 3(a) a large time pulse of $t_p=1000/\omega_z$ leads to efficient TWT, with the BEC moving smoothly from well 1 to well 3 with a minimal occupation of well 2. In Fig. 3(b), however, a significantly reduced pulse time of $t_p=14/\omega_z$ breaks adiabaticity causing inefficient transfer, with a significant population in well 2.

We now consider the possibility of producing efficient TWT in a realistic BEC system. We performed simulations of the full 3D GPE. Since strong nonlinear interactions suppress TWT, we focus on a system with weak interaction strength, i.e. a small *s*-wave scattering length a and low atom number N_T. Our simulations are based on recent ^{7}Li soliton experiments [26,27]. These experiments have two key advantageous features. First, the experiments worked with low atom number, with typically several thousand atoms in the condensate. Second, the experiments employed a Feshbach resonance to control the *s*-wave scattering length, allowing low attractive scattering lengths of the order $a=-0.1$ nm. In principle, similar experiments could probe the high fidelity parameter space of g and t_p.

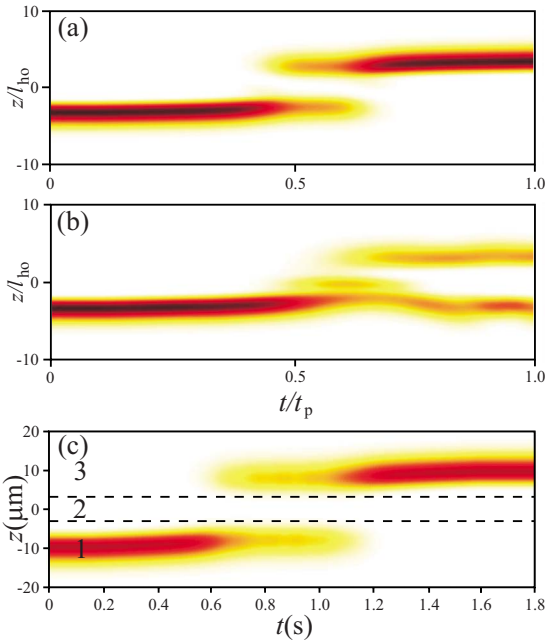

FIG. 3. (Color online) Dynamics of the system according to the 1D GPE. (a) Carpet plot showing the evolution of condensate density (dark=high density, light=low density) for an effective 1D interaction parameter of $g_{1D}=0.31$ and a pulse time of $t_p=1000/\omega_z$. (b) As (a) but for a small pulse time of $t_p=14/\omega_z$. Note the breakdown of the adiabatic transfer. (c) Evolution of the radially integrated axial density for the *counter-intuitive* protocol for a realistic BEC of 2000 ^{7}Li atoms with attractive interactions $a=-0.2$ nm. The horizontal dashed lines correspond to the center of the Gaussian barriers $\pm z_0$. We assume $\omega=2\pi\times 40$ Hz, $\sigma=1$ μm, $z_0=3$ μm, $V_{\max}=100\,\hbar\omega$, and $V_{\min}=5\,\hbar\omega$.

We consider $N_T=2000$ and $a=-0.2$ nm, and realistic parameters for our trapping system: $\omega_r=\omega_z=2\pi\times 40$ Hz, $\sigma=1$ μm, $V_{\max}=100\,\hbar\omega$, $V_{\min}=5\,\hbar\omega$, and $z_0=3$ μm. The BEC dynamics under the counter-intuitive protocol and for a pulse time of $t_p=400\ \omega^{-1}=1.6$ s and a pulse delay of $\tau=0.16$ s are presented in Fig. 1(b) as chronological frames of an isosurface of BEC density [25] and in Fig. 3(c) as a carpet plot of the radially integrated axial density. For these parameters we clearly see efficient TWT, i.e. the 2000 ^{7}Li atoms are adiabatically transported a distance of approximately 20 μm with negligible occupation of well 2. Crucially, the time scale for this process is just under 2 s, which is the lifetime of such condensates [27]. These results have a fidelity $\epsilon=0.985$, which is limited by the maximum occupation of well 2 during the transfer, where well 2 is defined as the spatial region $[-z_0,z_0]$. However, defining well 2 as the classically allowed

region between $-z_0$ and z_0 where the chemical potential of the initial state is less than $V(\mathbf{r},t)$. For this definition the maximum atom number at any time that occupies this classically allowed region is less than $0.01N_T$ ($\epsilon > 0.99$).

We have also simulated the dynamics of this system for the *intuitive* protocol, where the first barrier is pulsed before the second barrier. Under this protocol a macroscopic occupation, $0.15N_T$, of well 2 during the transfer is predicted. Hence, a straightforward experimental confirmation of TWT is to reverse the pulses and compare the condensate density in the middle well through the pulse sequence [9].

In conclusion we propose a protocol for the transport of BECs in three-well systems. This protocol enables the adiabatic transport of a macroscopic BEC such that the transient occupation of the intermediate well is heavily suppressed: transport without transit. In particular, we have shown that this works within both a three-mode approach and the mean-field GPE approximation. We have mapped out the parameter space for which we expect TWT to occur. Specifically, we predict the TWT of an interacting BEC of 2000 ^{7}Li atoms a macroscopic distance of 20 μm over a time scale of 1.8 s. This phenomenon is not only of interest from the viewpoint of testing the *wave* nature of a BEC, but also paves the way for a method of control in atom optical devices. Future extensions to this work include the examination of non–mean-field effects, such as quantum fluctuations [28], and systems with more than three wells [29].

The authors acknowledge useful discussions with Simon Devitt and David Jamieson. This work is funded by the Australian Research Council (ARC). J.H.C., A.D.G., and L.C.L.H. are also supported by the U.S. National Security Agency, the Australian Government and the Army Research Office under Contract No. W911NF-04-1-0290. Additionally, A.D.G. acknowledges ARC for financial support (DP0880466); L.C.L.H. acknowledges ARC for financial support (DP0770715).

[1] J. Oreg, F. T. Hioe, and J. H. Eberly, Phys. Rev. A **29**, 690 (1984).
[2] J. R. Kuklinski, U. Gaubatz, F. T. Hioe, and K. Bergmann, Phys. Rev. A **40**, 6741 (1989).
[3] U. Gaubatz *et al.*, J. Chem. Phys. **92**, 5363 (1990).
[4] K. Bergmann, H. Theuer, and B. W. Shore, Rev. Mod. Phys. **70**, 1003 (1998).
[5] M. Weitz, B. C. Young, and S. Chu, Phys. Rev. Lett. **73**, 2563 (1994).
[6] R. Wynar *et al.*, Science **287**, 1016 (2000).
[7] K. Winkler *et al.*, Phys. Rev. Lett. **98**, 043201 (2007).
[8] S. Longhi, J. Phys. B **40**, F189 (2007).
[9] S. Longhi, G. Della Valle, M. Ornigotti, and P. Laporta, Phys. Rev. B **76**, 201101(R) (2007).
[10] K. Eckert *et al.*, Phys. Rev. A **70**, 023606 (2004).
[11] K. Deasy *et al.*, e-print arXiv:quant-ph/0611174.
[12] J. Siewert and T. Brandes, Adv. Solid State Phys. **44**, 181 (2004).
[13] T. Ohshima *et al.*, e-print arXiv:quant-ph/0702019.
[14] P. Zhang, Q. K. Xue, X. G. Zhao, and X. C. Xie, Phys. Rev. A **69**, 042307 (2004).
[15] A. D. Greentree, J. H. Cole, A. R. Hamilton, and L. C. L. Hollenberg, Phys. Rev. B **70**, 235317 (2004).
[16] J. Fabian and U. Hohenester, Phys. Rev. B **72**, 201304(R) (2005).
[17] L. C. L. Hollenberg, A. D. Greentree, A. G. Fowler, and C. J. Wellard, Phys. Rev. B **74**, 045311 (2006).
[18] J. H. Cole, A. D. Greentree, S. D. Sarma, and L. C. L. Hollenberg, e-print arXiv:0802.2398, Phys. Rev. B (to be published).
[19] E. M. Graefe, H. J. Korsch and D. Witthaut, Phys. Rev. A **73**, 013617 (2006).
[20] G.-F. Wang, D. F. Ye, L. B. Fu, X. Z. Chen, and J. Liu, Phys. Rev. A **74**, 033414 (2006).
[21] B. Liu, L. B. Fu, S. P. Yang, and J. Liu, Phys. Rev. A **75**, 033601 (2007).
[22] The nonlinear interaction parameter in the mode analysis, g_m, can be considered as being similar to the interaction parameter, g, in the GPE.
[23] Y. Shin *et al.*, Phys. Rev. Lett. **92**, 050405 (2004).
[24] T. Schumm *et al.*, Nat. Phys. **1**, 57 (2005).
[25] See EPAPS Document No. E-PLRAAN-77-R10806 for the exact form of $V_{12}(t)$ and $V_{23}(t)$ used and the equivalent plots shown in Figs. 2(c) and 2(d), calculated using the one-dimensional GPE, and for a movie of the isosurface plot. For more information on EPAPS, see http://www.aip.org/pubservs/epaps.html.
[26] L. Khaykovich *et al.*, Science **296**, 1290 (2002).
[27] K. E. Strecker *et al.*, Nature (London) **417**, 150 (2002).
[28] P. Deuar and P. D. Drummond, Phys. Rev. Lett. **98**, 120402 (2007).
[29] A. D. Greentree, S. J. Devitt, and L. C. L. Hollenberg, Phys. Rev. A **73**, 032319 (2006).